Journal of Hydrology 602 (2021) 126734

Contents lists available at ScienceDirect

Journal of Hydrology

journal homepage: www.elsevier.com/locate/jhydrol

Research papers

Experimental and modeling investigation of pumping from a fresh groundwater lens in an idealized strip island

Yuening Tang [a], Min Yan [b], Xiaoxiong Wang [c], Chunhui Lu [b,*], Jian Luo [a,*]

[a] School of Civil and Environmental Engineering, Georgia Institute of Technology, GA 30332, USA
[b] State Key Laboratory of Hydrology-Water Resources and Hydraulic Engineering, Hohai University, Nanjing, China
[c] Department of Chemical and Environmental Engineering, Yale University, New Haven, CT 06520, USA

ARTICLE INFO

This manuscript was handled by Huaming Guo, Editor-in-Chief

Keywords:
Groundwater lens
Optimal pumping
Strip island

ABSTRACT

Groundwater lens floating on the seawater in surficial coastal aquifers is an important freshwater supply for small island inhabitants. This study addresses an unanswered, simple but important question for groundwater resources management in small islands: how much freshwater can be sustainably withdrawn from a groundwater lens in small islands. We derive an approximate analytical solution to describe the freshwater-seawater sharp interface profile in an idealized strip island subject to a pumping well located at the domain center to determine the critical or maximum allowable pumping rate that prevents saltwater upconing. A simple formula of the critical pumping rate is provided as a function of hydrogeologic parameters, including the recharge rate, densities, hydraulic conductivity and well penetrating depth. It shows that the critical pumping rate increases linearly with the recharge rate and decreases linearly with the hydraulic conductivity and the squared well penetrating depth. Laboratory visualization experiments and numerical simulations were conducted to validate the derived analytical solution. Results indicate that the maximum pumping rate can be as high as 50% of the total recharge for a single well located at the top of the domain center. Our solutions and results provide useful insights for sustainable groundwater management in small islands and can potentially render significant social and economic impact for inhabitants on small islands.

1. Introduction

Inhabitants on small islands often face the stress of insufficient freshwater resources due to the lack of natural surface water reservoirs. Groundwater provides an important freshwater supply for small islands. In surficial coastal aquifers, fresh groundwater floats as a lens above the seawater due to density difference. A transition zone can be delineated between the freshwater and seawater. In many cases, the transition zone may be approximated as a sharp interface when it is relatively thin compared with the aquifer thickness (Lu et al., 2009; Lu and Luo, 2010; Lu and Luo, 2014; Rathore et al., 2018a; Rathore et al., 2018b; Rathore et al., 2020). The elevation or position of the interface determines the volume of freshwater potentially available for withdrawal, which generally fluctuates with the long-term change pattern of recharge intensity (Tang et al., 2020). The interface equilibrium between freshwater and seawater can be broken when excessive freshwater is withdrawn from water supply wells, causing an upward movement of the interface towards the pumping well, commonly referred as upconing (Asghar et al., 2002; Bear, 2012). Thus, for sustainable groundwater resources management on small islands, a key is the determination of critical or maximum pumping rates that can be applied without inducing saltwater upconing into water production wells.

Research of saltwater upconing has a long history. Muskat (1938) first provided an approximate solution for steady state flow to a pumping well above a freshwater-seawater interface by assuming that the interface moves only a small distance compared with the original spacing between the well and interface. Since then, several analytical solutions based on the sharp-interface assumption have been developed to investigate the pumping-induced upward movement of the freshwater-saltwater interface (Dagan and Bear,1968; Strack, 1972; Zhang and Hocking, 1996; Dagan and Zeitoun, 1998; Bower et al., 1999; Zhang et al., 2009). Numerical modeling of saltwater upconing generally solves coupled variable-density flow and transport, including the most popular computer codes SEAWAT and SUTRA, both developed by U.S. Geological Survey (Langevin et al., 2003; Voss and Provost, 2002). The major difference between numerical simulations and sharp-

* Corresponding authors.
E-mail addresses: clu@hhu.edu.cn (C. Lu), jian.luo@ce.gatech.edu (J. Luo).

https://doi.org/10.1016/j.jhydrol.2021.126734
Received 20 April 2021; Received in revised form 16 July 2021; Accepted 21 July 2021
Available online 27 July 2021

interface analytical solutions is the effects of hydrodynamic dispersion, which yields a variable-density transition zone between freshwater and seawater (Rubin and Pinder, 1977; Wirojanagud and Charbeneau, 1985; Reilly and Goodman, 1987; Ma et al., 1997; Zhou et al., 2005; Lu et al., 2019). For sharp-interface solutions, the critical pumping rate is solely determined by the position of cone apex, while for a variable-density transition zone the concentration in the pumping well or a specified iso-concentration line needs to be defined to determine the critical pumping rate. Experimental studies (Abdoulhalik and Ahmed, 2018; Oswald et al., 2002; Werner et al., 2009) and field investigation were also conducted to study the behavior of saltwater upconing (Schmork and Mercado, 1969; Gopinath et al., 2016; Houben and Post, 2017).

Although saltwater upconing has been studied for many years, the research of upconing in small islands is limited. There are two major differences regarding the problem conceptualizations between the previous studies and in small islands. Firstly, a typical assumption in previous studies is that the initial interface is horizontally infinite or semi-infinite, which may only be valid for describing local upconing behavior on the top of a large-scale seawater intrusion wedge or a lens interface in large islands. In small islands, the sea boundary has significant impact to shape the lens interface profile. Secondly, most previous studies assumed horizontal inflow freshwater flux from side boundaries to supply the withdrawal, while the vertical recharge from the ground surface is considered as the freshwater source for the groundwater lens in small islands. Therefore, most of previous studies discussed above cannot be directly applied to investigate the upconing problem of the freshwater-seawater interface in a small island and to determine the critical groundwater withdrawal rate from a groundwater lens.

There are also extensive studies on freshwater lens behavior in small islands under varying conditions by analytical, numerical, and physical models (Bedekar et al., 2019; Chui and Terry, 2012; Chui and Terry, 2015; Dose et al., 2014; Fetter, 1972; Houben and Post, 2017; Ketabchi et al., 2014; Memari et al., 2020; Post et al., 2018; Schneider and Kruse, 2006; Stoeckl and Houben, 2012; Stoeckl et al., 2015; Stoeckl et al., 2016; Vacher, 1988). However, few studies have been conducted to investigate the upconing problem of a freshwater lens interface to determine the critical pumping rate in small islands (Banerjee and Singh, 2011; Kura et al., 2014; Piscopo et al., 2020). Many fundamental scientific questions remain unanswered. For example, the simplest but most important question is how high the pumping rate can be for withdrawing freshwater from the groundwater lens in a small island. The answer to this question is very useful for sustainable groundwater management, and can potentially render significant social and economic impact for inhabitants on small islands. To this end, the present study focuses on a single pumping well in a small strip island. We provide an explicit analytical formula for the first time to determine the critical pumping rate of a pumping well located at the center of an island and the steady-state lens interface profile under vertical recharge and groundwater withdrawal. The analytical solution is validated by numerical models and laboratory visualization experiments. Sensitivity analysis is conducted to investigate the critical pumping rate under various hydrogeological conditions.

2. Conceptual model

Fig. 1 shows the vertical cross section of a typical fresh groundwater lens in a small island. Strip islands are considered here for simplicity. The island length is assumed much longer than its width, $2W$ [L], allowing us to simplify the problem to the two-dimensional vertical section. The aquifer is homogeneous, isotropic and unconfined with a freshwater hydraulic conductivity, K [L/T]. Seawater boundaries at both domain sides are assumed constant-head. The impact of tidal activities is not considered by assuming that the interface fluctuations due to high-frequency tidal activities are negligible (Tang et al., 2020). A constant and uniformly distributed recharge rate, ω [L/T], is applied along the surface. The transition zone between the seawater and freshwater is

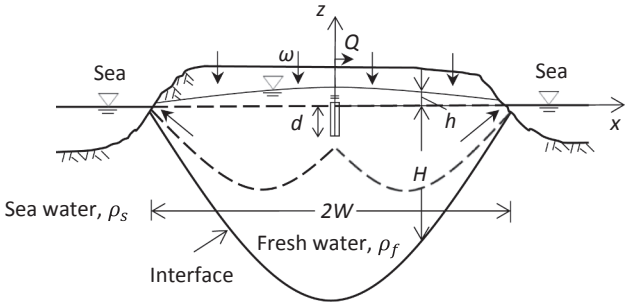

Fig. 1. Two-dimensional conceptual model for the groundwater lens in a small strip island with recharge at the top and pumping at the center.

approximated as a sharp interface. This simplification was initially validated by Muskat (1938) and has been widely used by numerous researchers in coastal aquifers without high heterogeneity and large dispersion (Lu et al., 2009; Lu and Luo, 2014). Freshwater is separated by this interface and floats above the seawater in the form of lens.

We define the thickness of lens as the distance from the interface to the sea level, H. We shall notice that the actual freshwater thickness is the distance from the interface to the water table, i.e., $H + h$, shown in Fig. 1. A simple relationship can be established between H and h according to the Ghyben-Herzberg relationship. The interface is symmetric with the maximum thickness at the center, $x = 0$. The aquifer is assumed much thicker than the maximum thickness of the lens so that the lens is fully developed. Fig. 1 schematically shows the shape of the lens under groundwater withdrawal from a single well. The pumping well is placed at the center of the lens with a penetration depth of d [L] to achieve the maximum pumping rate. Since the conceptual model is two-dimensional, the pumping well actually represents a drain or a line sink (Strack, 1972; Zhang and Hocking, 1996; Zhang et al., 2009). The lens interface beneath the well rises in response to pumping, changing the interface to an 'ω' shape. With the increase of the pumping rate, the center of the interface moves toward the well. A critical pumping rate can be defined as the maximum pumping rate that can be applied to prevent the interface peak from penetrating into the well, i.e., the peak remains stable as long as the pumping rate does not exceed the critical pumping rate.

3. Approximate analytical solution

3.1. Groundwater lens interface profile

For the conceptual model shown in Fig. 1, the pumping rate is assumed low so that the upconing has not penetrated into the pumping well. Due to symmetry, the analytical model describes the half island as the whole domain. By neglecting the storage effect of water expansion and aquifer compaction, i.e., the net water flux into the groundwater lens controls the lens shape and volume (Hantush, 1968), we have the continuity equation:

$$\frac{\partial q_x}{\partial x} + \frac{\partial q_z}{\partial z} = 0 \tag{1}$$

where x [L] is the distance from the center; z [L] is the vertical coordinate; q_x [LT^{-1}] and q_z [LT^{-1}] are specific or Darcy's velocities at x and z-direction, respectively.

We can integrate Eq. (1) over the freshwater lens thickness along the z-direction of the lens cross section, i.e., the vertical direction (as shown in Fig. 1) and the positive upward direction, and apply Leibnitz's rule:

$$\frac{\partial\left(\int_{-H}^{h} q_x dz\right)}{\partial x} - q_x(-H)\frac{\partial H}{\partial x} - q_x(h)\frac{\partial h}{\partial x} + q_z(h) - q_z(-H) = 0 \tag{2}$$

$$q_z(h) = \frac{\varepsilon dh}{dt} \tag{3}$$

$$q_z(-H) = -\frac{\varepsilon dH}{dt} \tag{4}$$

where ε [−] is the porosity.

Substituting Darcy's law $q_x = -K\frac{\partial h}{\partial x}$ and the Ghyben-Herzberg relationship, $h = \delta H$, into Eqs. (3) and (4) and applying the linearization method of the Boussinesq equation (Hantush, 1968; Bear, 2012), the governing equation is derived as:

$$\frac{K\delta\overline{H}}{\varepsilon}\frac{\partial^2 H^2}{\partial x^2} = \frac{\partial H^2}{\partial t} \tag{5}$$

where t [T] is the time;$\delta = (\rho_s - \rho_f)/\rho_f$; ρ_s [M/L^3] and ρ_f [M/L^3] are seawater and freshwater density, respectively; $\overline{H}$ [L] is the average of the areal distribution of the depth.

According to Dupuit assumption and the assumption that the hydraulic head along a vertical plane is the average value between the water table and interface, the well discharge q [L^{2}T^{-1}] through a vertical plane can be written as (Fetter, 1972; Bear, 2012; Rathore et al., 2020):

$$q = -K(h+H)\frac{\partial h}{\partial x} \tag{6}$$

We can rearrange Eq. (6) as:

$$q = -K(\delta+1)\delta\frac{\partial H^2}{2\partial x} \tag{7}$$

At $x = 0$, the interpretation of pumping point is analogous to Eq. (7). The only difference is that we consider the flow from both sides of the vertical plane. Thus, at the pumping point, we have a Neumann boundary (Hantush, 1968):

$$\frac{\partial H^2(0,t)}{\partial x} = \frac{-q}{\delta(1+\delta)K} \tag{8}$$

The sea level is assumed constant:

$$H^2(W,t) = 0 \tag{9}$$

The transient-state solution can be derived for Eq. (5) given the average depth, which is not needed for the steady state. The steady-state solution of H^2 can be obtained as:

$$H^2(x) = \frac{-q}{\delta(1+\delta)K}(x - W) \tag{10}$$

Eq. (10) provides the solution to the interface profile subject to groundwater pumping. For the impact of recharge, the steady state solution of the lens interface under a recharge rate ω is given by (Fetter, 1972):

$$H^2(x) = \frac{\omega\left(W^2 - x^2\right)}{\delta(1+\delta)K} \tag{11}$$

Since H^2 is approximated by a linear system, Eq. (5), we can obtain the steady-state interface profile under both pumping and recharge by superposing Eq. (10) and Eq. (11):

$$H^2(x) = \frac{\omega\left(W^2 - x^2\right)}{\delta(1+\delta)K} + \frac{q}{\delta(1+\delta)K}(x - W) \tag{12}$$

3.2. Critical pumping rate

The above approximate solution assumes that the pumping well is located at the surface, i.e., the upconing peak can reach the top at the critical pumping rate. Thus, by setting $H = 0$ at $x = 0$ in Eq. (12), we can get the critical pumping rate for the well at the top at the center of the island:

$$q_{\max} = \omega W \tag{13}$$

For a pumping well penetrating into the aquifer, the saltwater can be prevented from entering the well if the steady-state interface elevation in the pumping state is lower than the location of the well screen. Thus, the critical pumping rate can be determined by specifying the vertical distance from the well screen to the bottom of the pre-pumping lens as the maximum allowed interface elevation. This method was applied in previous studies to obtain the critical pumping rate for a partially-penetrating well (Chandler and McWhorter, 1975). For the analytical modeling approach, the critical pumping rate can be calculated directly by setting the left side of Eq. (12) equal to the squared well depth at $x = 0$, i.e., $H^2(x = 0) = d^2$. Thus, we obtain:

$$q_{\max} = \omega W - \frac{\delta(1+\delta)Kd^2}{W} \tag{14}$$

Eq. (14) includes the case of well at the surface by letting $d = 0$.

The analytical solution also enables us to generalize the problem with the following dimensionless variables:

$$H^* = \frac{H}{W},\ \omega^* = \frac{\omega}{K},\ \overline{H}^* = \frac{\overline{H}}{W},\ t^* = \frac{Kt}{W\varepsilon},\ x^* = \frac{x}{W},\ d^* = \frac{d}{W},\ q^* = \frac{q}{KW} \tag{15}$$

Eqs. (12) and (14) can be written as:

$$H^{*2}(x^*) = \frac{\omega^*(1 - x^{*2})}{\delta(1+\delta)} + \frac{q^*}{\delta(1+\delta)}(x^* - 1) \tag{16}$$

$$q^* = \omega^* - \delta(1+\delta)d^{*2} \tag{17}$$

Eq. (17) indicates that the dimensionless critical pumping rate is controlled by two parameters, the dimensionless recharge rate and the well penetrating depth.

To investigate how much water can be withdrawn from the total recharge, we define the critical pumping ratio, η, by normalizing the critical pumping rate with the total recharge rate, $\Omega = 2W\omega$.

$$\eta = \frac{q}{\Omega} = \frac{q^*}{2\omega^*} = \frac{1}{2} - \frac{\delta(1+\delta)d^{*2}}{2\omega^*} \tag{18}$$

which indicates that the maximum or critical pumping rate for a well located at the aquifer top, i.e., $d = 0$, is half of the total recharge rate.

4. Laboratory visualization experiments

4.1. Experiment setup

Following the conceptual model, we conducted laboratory experiments to visualize the interface upconing. Fig. 2 shows the configuration parameters and real image of the experimental tank system. An acrylic glass box of 60 cm length, 18 cm height and 1 cm width was used as a sand tank to simulate the cross-section of a strip island, with coarse sand filled to a height of 17 cm (Fig. 2). The left and right reservoirs used to represent the seawater boundary were connected to the glass box through a 5 cm long channel and contained seawater with water level 15 cm above the tank bottom. Also, the two reservoirs were big enough to diminish seawater surface fluctuations due to outflow and connected to each other to keep the water level equal for both sides. To avoid mixing between freshwater and saltwater, four drippers, at the rate of recharge rate, were arranged on each side to pump the mixture from the upper port. Surface recharge was supplied by a multi-channel peristaltic pump (Longerpump BT100-1L) through twelve freshwater dippers. Recharge rate were set to 0.12, 0.28, 0.56 cm/min, respectively, equal to 0.6, 1.4 and 2.8 mL/min per dipper. A stainless steel pipe with a diameter of 2 mm was inserted into the flow tank at the center to simulate the horizontal well, from the back to the front. The total length of the steel pipe was 2.5 cm, of which 1 cm was covered with small notches, and the rest was located outside the sandbox and connected to

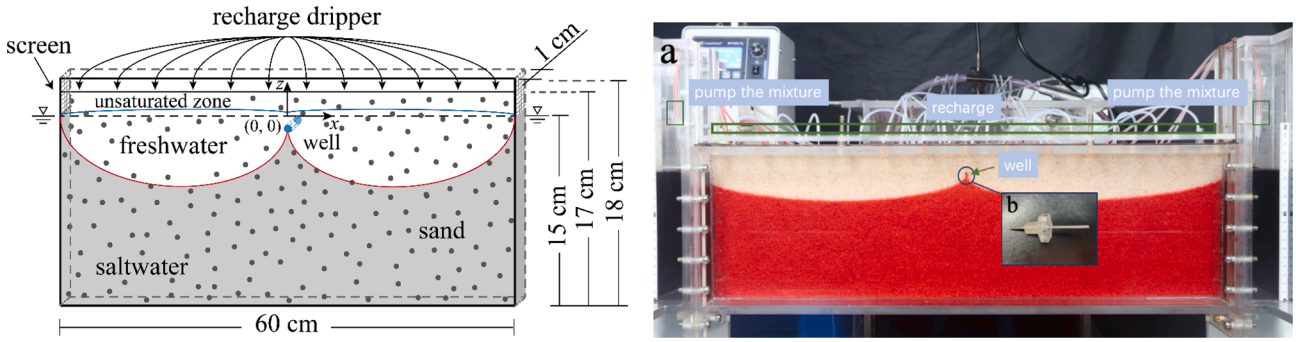

Fig. 2. Sand tank configurations for laboratory visualization experiments.

another peristaltic pump through a rubber tube at the back for well pumping. The steel pipe was placed at 0, 2.5 and 5 cm below sea level for different experiments. A density meter was used to determine fresh and saline water densities, which were set to 998 and 1024.9 kg/m^3, respectively. The density meter also monitors the concentration of pumping water. A tracer dye was added to the saltwater for visualization, and the density was checked to ensure this led to no measurable change. All experiments were photographed at 10-minute intervals using a digital camera (Canon EOS 800D).

Coarse sands were filled uniformly in the tank. Several experiments were conducted in-situ to determine the hydraulic conductivity value. First, we keep the right side as inlet side of specified-flux Q, and the left side as an outlet side of specified-head h_{out}. After reaching the steady state, the head at the right side was recorded as h_{in}. Then, the K value can be calculated from:

$$K = \frac{4QW}{W_T(h_{in}^2 - h_{out}^2)} \tag{19}$$

where W and W_T are the half width and thickness of sand tank, equal to 30 cm and 1 cm respectively according to our experiment setup. Four sets of Q values were applied, and corresponding K values were estimated from the equation above. We adopted the arithmetic means, 200 cm/min, as the K value in both analytical solutions and numerical modeling. Similar K values were used in previous studies of laboratory lenses (Dose et al., 2014; Lu et al., 2019; Stoeckl et al., 2015; Yan et al., 2021). The porosity value was measured through the water saturation method (Fetter, 2018), and determined to be 0.38 (Yan et al., 2021).

4.2. Experimental validation results

Fig. 3 compares the interface profiles given by Eq. (12) and the laboratory visualization experiments under the critical pumping rate determined by Eq. (14) for wells located at the tank top and partially penetrating into the tank media. Thin interfaces were created in the homogeneous sand (Abarca and Clement, 2009; Lu et al., 2013). All cases showed good agreement of interface profiles between experimental results and the approximate analytical solutions. We used three different recharge rates (Fig. 3a–c) for the water withdrawal at the top of the tank. The volume of the freshwater lens or the interface thickness at the domain center increases with the recharge rate. Correspondingly, a higher water withdrawal rate can be achieved for a higher recharge rate. Given a constant recharge rate, the total freshwater volume available for withdrawal is constant. However, the critical pumping rate decreases with the well penetration depth (Fig. 3d – 3f), because the interface upconing peak is limited to the pumping depth.

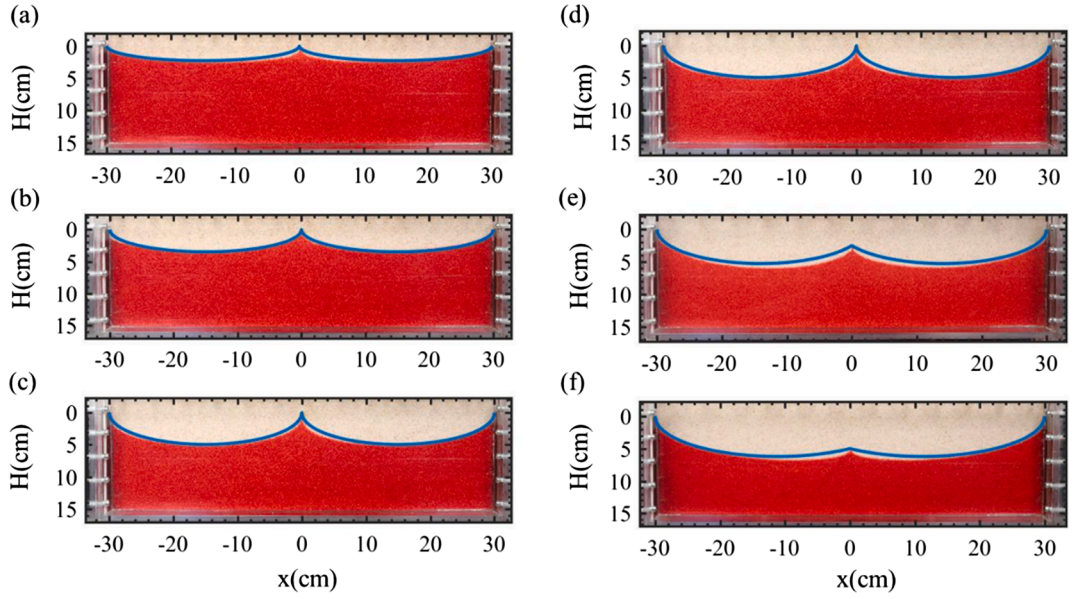

Fig. 3. Comparison of steady-state interfaces between analytical solution and laboratory results under the critical pumping at the tank top for the recharge rate ω of (a) 0.12 cm/min, (b) 0.28 cm/min, and (c) 0.56 cm/min, and under the critical pumping rate for a constant recharge rate ω of 0.56 cm/min at the well depth d of (d) 0 cm, (e) 2.5 cm, and (f) 5 cm. The blue lines are analytical solutions. The hydraulic conductivity K is 200 cm/min. The half width W is 30 cm. (For interpretation of the references to colour in this figure legend, the reader is referred to the web version of this article.)

5. Numerical simulations

5.1. Setup of numerical cases

The approximate analytical solution is also validated by field-scale numerical cases simulated using SEAWAT (Langevin et al., 2003), which combines MODFLOW and MT3DMS to simulate variable-density flow. Table 1 lists typical hydrogeologic and geometric parameters for a base field-scale numerical model. Recharge rates and well penetrating depths are varied to investigate the sensitivity. Each grid of the 600 m × 150 m domain is 1 m × 1 m. We compare the magnitude of critical pumping rates and the corresponding upconing interface profiles in the case of various recharge rates and well depths for numerical simulations and analytical solutions in the dimensionless form in the next section. We shall notice that it is not convenient to estimate the critical pumping rate by numerical modeling. Because the pumping rate needs to be predefined for numerical simulations, one can only try different pumping rates and visualize the concentration distributions or obtain the concentration profile at the pumping well to determine the maximum pumping rate that can maintain a stable interface without penetrating into the well. We use 1% as the salt concentration threshold to obtain the critical pumping rate in the numerical model. One may define other threshold values, such as the 50% concentration contour line (Rathore et al., 2018a; Reilly and Goodman, 1987), which may yield similar behavior for thin lens interfaces.

5.2. Numerical case validation

Fig. 4(a) shows the field-scale numerical simulation results at the critical pumping rates for the recharge rate ω^* at 10^{-4}, 5×10^{-4}, and 10^{-3} for the pumping well located at the top of the aquifer. Symbols represent the contour lines of 1% salt concentration normalized by the seawater concentration for numerical simulations. The interface profiles given by the approximate analytical solution match numerical simulations in all cases. In general, a higher recharge rate leads to a deeper interface, indicating a larger freshwater volume stored in the aquifer. Moreover, the upconing peak under the critical condition is located just below the well, implying a critical interface rise ratio of 1. The interface rise ratio is defined as the interface upconing height normalized by the distance between the well screen and the original lens profile. In infinite or semi-infinite horizontally flow domain without the vertical recharge, the critical rise ratio was found around 0.25–0.9 (Bower et al., 1999; Motz, 1992; Werner et al., 2009). The difference is that the constant recharge of the lens from the top inhibits the upward movement of the interface and leads to a more stable interface than the cases with the recharge flow from side boundaries.

Fig. 4(b) compares the analytical solution and 1% concentration contour lines in the numerical simulation for partially penetrating wells. The lens is assumed to be in a steady state before pumping. The critical pumping rate q^* is 8×10^{-4} and 5×10^{-4} for the dimensionless well depth d^* at 0.09 and 0.14, respectively. The critical pumping rate is reduced when the well penetrates deeper because a deeper well leads to a smaller allowed interface upconing. Fig. 6 clearly shows that the analytical solution provides excellent approximation of the numerical solution for different recharge rates and penetrating wells.

Table 1
Hydrogeologic and geometric parameters used in the numerical model for validating the approximate analytical solution.

Parameter	Value
Height	150 m
Width, $2W$	600 m
Hydraulic conductivity, K	10^{-4} m/s
Porosity, ε	0.1
Molecular diffusion	3.56×10^{-9} m^2/s
Longitudinal Dispersivity	0.01 m
Freshwater density	1000 kg/m^3
Seawater density	1025 kg/m^3

5.3. Sensitivity analysis

5.3.1. Effects of recharge rate and well penetration depth

Eqs. (14) and (17) provide simple first-order relationships between the critical pumping rate and hydrogeological and well parameters. That is, the critical pumping rate q^* linearly increases with the recharge rate and linearly decreases with the squared well penetration depth. Fig. 5 shows that these first-order relationship are well confirmed by the numerical simulations, especially at high recharge rates. The reason is that the salt concentration at the pumping well is more likely to be affected by the transition zone between freshwater and seawater when the lens thickness becomes thinner under a lower recharge rate.

From Fig. 5(b), we should note that there is a limit for the well depth, at which the critical pumping rate is zero. By letting the left side of Eq. (14) be zero, we can have the depth limit: $d = \sqrt{\frac{\omega W^2}{\delta(1+\delta)K}}$, which is also the maximum thickness of the lens center.

5.3.2. Effects of hydraulic conductivity

Eq. (14) indicates that the critical pumping rate decreases linearly with the hydraulic conductivity. Thus, the recharge rate and hydraulic conductivity have opposite impact on the critical pumping rate. Such opposite impact was also observed in previous studies (Greskowiak et al., 2013; Ketabchi et al., 2014; Vacher, 1988). Another interesting observation given by Eq. (14) is that the critical pumping rate is independent of hydraulic conductivity if the pumping is applied at the aquifer top, i.e., $d = 0$. This case is common for a shallow well in a relatively thick groundwater lens. To verify this finding, we consider four cases for the well located at the top:

$$\text{Case1: } \omega = 10^{-8}\tfrac{m}{s},\ K = 10^{-3}\tfrac{m}{s},\ \omega^* = 10^{-5}$$
$$\text{Case2: } \omega = 10^{-7}\tfrac{m}{s},\ K = 10^{-3}\tfrac{m}{s},\ \omega^* = 10^{-4}$$
$$\text{Case3: } \omega = 10^{-8}\tfrac{m}{s},\ K = 10^{-4}\tfrac{m}{s},\ \omega^* = 10^{-4}$$
$$\text{Case4: } \omega = 10^{-7}\tfrac{m}{s},\ K = 10^{-4}\tfrac{m}{s},\ \omega^* = 10^{-3}$$

Eq. (16) shows that the lens interface under the critical pumping rate only depends on ω^*. This is verified by the interface profiles under the critical pumping rates shown in Fig. 6, where Cases 2 and 3 have the same ω^* (from different combination of ω and K) and almost overlapped interface profiles. Case 4 with a larger ω^* produces a thicker lens and Case 1 with a smaller ω^* produces a thinner lens than those of Cases 2 or 3. It also demonstrates that using the ratio between recharge rate and hydraulic conductivity as the dimensionless form of ω^* is valid. Thus, Cases 2 and 3 have the same dimensionless critical pumping rate, q^*, however, due to the different recharge rates, the actual pumping rates are an order of magnitude difference. Moreover, Cases 2 and 4 have different hydraulic conductivity, i.e., 10^{-3} m/s and 10^{-4} m/s, but the same actually pumping rate in the numerical simulations, validating the conclusion from Eq. (14) that the magnitude of hydraulic conductivity has no impact on the actual critical pumping rate for a well located at the top.

6. Conclusion

This study addresses a simple but important question for groundwater resources management in coastal islands: how much freshwater can be withdrawn from a fresh groundwater lens in island aquifers? We present an idealized conceptual model with a single pumping well located at the center of a two-dimensional vertical cross section of a small strip island. An explicit analytical solution is derived to determine the critical pumping rate for groundwater withdrawal at different well

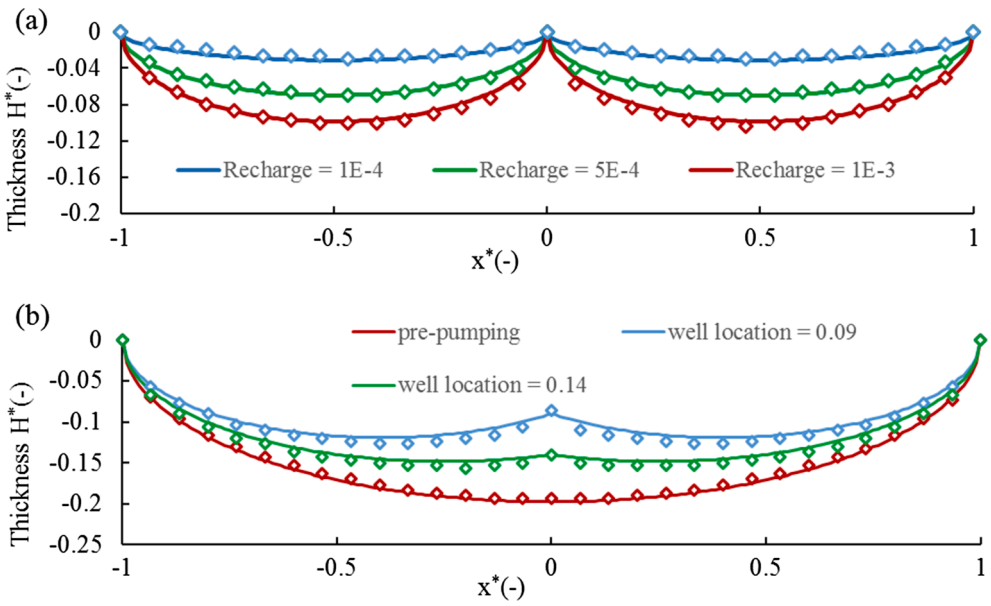

Fig. 4. Comparison of steady-state interfaces between the analytical solution and 1% isochlor from numerical simulations at the critical pumping rate. (a) Recharge rates ω^* of 10^{-4}, 5×10^{-4} and 10^{-3}. (b) Dimensionless well depths d^* of 0.09 and 0.14 with a constant recharge rate ω^* of 10^{-3}. The solid lines are analytical solutions and symbols are numerical simulations.

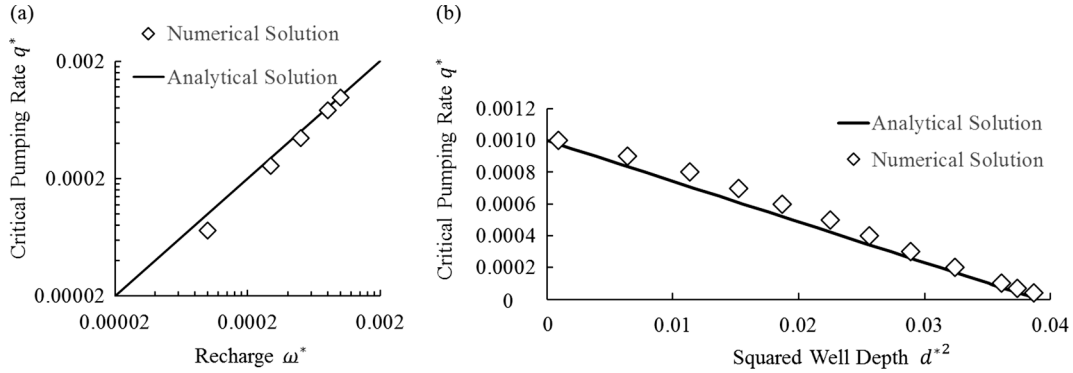

Fig. 5. Sensitivity analysis of the critical pumping rate q^* in terms of the recharger rate $\omega^*$and penetration depth d^*. (a) Linear relationship between q^* and ω^* for the pumping well located at the top, $d^* = 0$. (b) Linear relationship between q^* and squared well depth d^{*2} for the recharge rate ω^* of 10^{-3}.

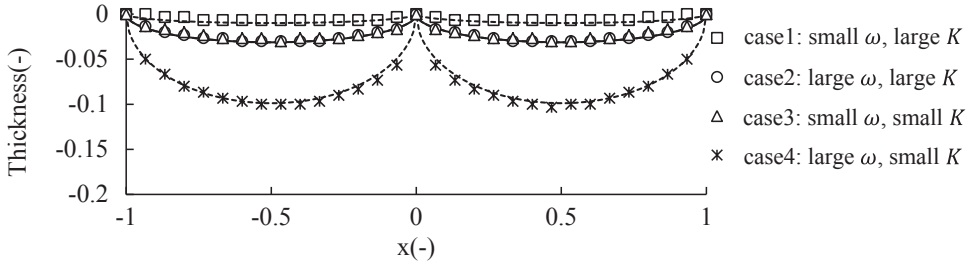

Fig. 6. Effects of hydraulic conductivity on the critical pumping rate by analytical and numerical simulations. Comparison of steady-state interfaces between the analytical solution and 1% isochlor from the numerical simulation under the critical pumping rate. The dash lines are analytical solutions and symbols are numerical simulations.

penetration depth. The analytical solution indicates that the critical pumping rate linearly increases with the recharge rate and linearly decreases with the hydraulic conductivity and the squared well penetrating depth. Numerical simulations and laboratory visualization experiments are conducted to validate the results obtained by the analytical solutions. We found that the maximum pumping rate of a well located at the aquifer top is not affected by hydraulic conductivity and can theoretically reach 50% of the total recharge in our idealized model. That is, a pumping rate greater than half of the recharge is not sustainable. One may use this information as simple guidance for groundwater withdrawal. For example, St. George island can extract about several millions of cubic meters of freshwater per year from the lens according to hydrogeological conditions and precipitation rates in the island (Schneider and Kruse, 2006).

There are several limitations with the derived solution and findings. In addition to the simplified hydrogeological settings, such as homogeneous thick aquifer, vertical section, and uniform recharge, etc., the critical pumping rate from the approximate analytical solution may not guarantee the pumped water is pure freshwater due to the sharp interface assumption. In particular, for islands with thick variable-density transitional zones, it may be necessary to use the breakthrough concentrations in the pumping well to determine the critical pumping rate. The pumping rate is also assumed to be constant, but in reality, it may vary in different seasons. In addition, we only consider a single pumping well. In the practical field, multiple wells are commonly used for pumping. This leads to another interesting problem: given a certain number of pumping wells, how should the wells be placed and what pumping rates should be assigned? This is a typical optimization problem for determining optimal pumping strategies in offshore coastal aquifers for maximizing the total pumping rate and preventing seawater intrusion. But this optimization problem has not been solved in island aquifers with the consideration of interface upconing. The research is underway to extend the current study of a single pumping well to the optimization of multiple wells in small islands. Nonetheless, our solutions and study provide very useful insights into the behavior of interface upconing and the impact of hydrogeologic conditions on critical pumping rates in small strip islands.

CRediT authorship contribution statement

Yuening Tang: Methodology, Investigation, Software, Validation, Formal analysis, Writing - original draft. **Min Yan:** Investigation, Writing - original draft. **Xiaoxiong Wang:** Methodology, Writing - review & editing. **Chunhui Lu:** Supervision, Methodology, Writing - review & editing. **Jian Luo:** Conceptualization, Methodology, Supervision, Writing - review & editing.

Declaration of Competing Interest

The authors declare that they have no known competing financial interests or personal relationships that could have appeared to influence the work reported in this paper.

Acknowledgement

We thank the two anonymous reviewers and editors, who helped improve the quality of the manuscript. Y. Tang gratefully acknowledges the partial financial support from China Scholarship Council.

References

Abarca, E., Clement, T.P., 2009. A novel approach for characterizing the mixing zone of a saltwater wedge. Geophys. Res. Lett. 36 (6), L06402.
Abdoulhalik, A., Ahmed, A.A., 2018. Transient investigation of saltwater upconing in laboratory-scale coastal aquifer. Estuar. Coast. Shelf Sci. 214, 149–160.
Asghar, M.N., Prathapar, S.A., Shafique, M.S., 2002. Extracting relatively-fresh groundwater from aquifers underlain by salty groundwater. Agric. Water Manag. 52 (2), 119–137.
Banerjee, P., Singh, V.S., 2011. Optimization of pumping rate and recharge through numerical modeling with special reference to small coral island aquifer. Phys. Chem. Earth. Parts A/B/C 36 (16), 1363–1372.
Bear, J., 2012. Hydraulics of Groundwater. Courier Corporation.
Bedekar, V.S., Memari, S.S., Clement, T.P., 2019. Investigation of transient freshwater storage in island aquifers. J. Contam. Hydrol. 221, 98–107.
Bower, J.W., Motz, L.H., Durden, D.W., 1999. Analytical solution for determining the critical condition of saltwater upconing in a leaky artesian aquifer. J. Hydrol. 221 (1-2), 43–54.
Chandler, R.L., McWhorter, D.B., 1975. Upconing of the salt-water–fresh-water interface beneath a pumping well. Groundwater 13 (4), 354–359.
Chui, T.F.M., Terry, J.P., 2012. Modeling fresh water lens damage and recovery on atolls after storm-wave washover. Groundwater 50 (3), 412–420.
Chui, T.F.M., Terry, J.P., 2015. Groundwater salinisation on atoll islands after storm-surge flooding: modelling the influence of central topographic depressions. Water Environ. J. 29 (3), 430–438.
Dagan, G., Bear, J., 1968. Solving the problem of local interface upconing in a coastal aquifer by the method of small perturbations. J. Hydraul. Res. 6 (1), 15–44.
Dagan, G., Zeitoun, D.G., 1998. Free-surface flow toward a well and interface upconing in stratified aquifers of random conductivity. Water Resour. Res. 34 (11), 3191–3196.
Dose, E.J., Stoeckl, L., Houben, G.J., Vacher, H.L., Vassolo, S., Dietrich, J., Himmelsbach, T., 2014. Experiments and modeling of freshwater lenses in layered aquifers: steady state interface geometry. J. Hydrol. 509, 621–630.
Fetter, C.W., 2018. Applied Hydrogeology. Waveland Press.
Fetter, C.W., 1972. Position of the saline water interface beneath oceanic islands. Water Resour. Res. 8 (5), 1307–1315.
Gopinath, S., Srinivasamoorthy, K., Saravanan, K., Suma, C., Prakash, R., Senthilnathan, D., Chandrasekaran, N., Srinivas, Y., Sarma, V., 2016. Modeling saline water intrusion in Nagapattinam coastal aquifers, Tamilnadu, India. Model. Earth Syst. Environ. 2 (1), 2.
Greskowiak, J., Röper, T., Post, V.E., 2013. Closed-form approximations for two-dimensional groundwater age patterns in a fresh water lens. Groundwater 51 (4), 629–634.
Hantush, M.S., 1968. Unsteady movement of fresh water in thick unconfined saline aquifers. Hydrol. Sci. J. 13 (2), 40–60.
Houben, G., Post, V.E.A., 2017. The first field-based descriptions of pumping-induced saltwater intrusion and upconing. Hydrogeol. J. 25 (1), 243–247.
Ketabchi, H., Mahmoodzadeh, D., Ataie-Ashtiani, B., Werner, A.D., Simmons, C.T., 2014. Sea-level rise impact on fresh groundwater lenses in two-layer small islands. Hydrol. Process. 28 (24), 5938–5953.
Kura, N.U., Ramli, M.F., Ibrahim, S., Sulaiman, W.N.A., Zaudi, M.A., Aris, A.Z., 2014. A preliminary appraisal of the effect of pumping on seawater intrusion and upconing in a small tropical island using 2D resistivity technique. Sci. World J. 2014.
Langevin, C.D., Shoemaker, W.B., Guo, W., 2003. MODFLOW-2000, the US Geological Survey Modular Ground-Water Model–Documentation of the SEAWAT-2000 Version with the Variable-Density Flow Process (VDF) and the Integrated MT3DMS Transport Process (IMT), 2003-426.
Lu, C., Cao, H., Ma, J., Shi, W., Rathore, S.S., Wu, J., Luo, J., 2019. A proof-of-concept study of using a less permeable slice along the shoreline to increase fresh groundwater storage of oceanic islands: analytical and experimental validation. Water Resour. Res. 55 (8), 6450–6463.
Lu, C., Chen, Y., Zhang, C., Luo, J., 2013. Steady-state freshwater–seawater mixing zone in stratified coastal aquifers. J. Hydrol. 505, 24–34.
Lu, C., Kitanidis, P.K., Luo, J., 2009. Effects of kinetic mass transfer and transient flow conditions on widening mixing zones in coastal aquifers. Water Resour. Res. 45 (12) https://doi.org/10.1029/2008WR007643.
Lu, C., Luo, J., 2010. Dynamics of freshwater-seawater mixing zone development in dual-domain formations. Water Resour. Res. 46 (11).
Lu, C., Luo, J., 2014. Groundwater pumping in head-controlled coastal systems: The role of lateral boundaries in quantifying the interface toe location and maximum pumping rate. J. Hydrol. 512, 147–156.
Ma, T.S., Sophocleous, M., Yu, Y.-S., Buddemeier, R.W., 1997. Modeling saltwater upconing in a freshwater aquifer in south-central Kansas. J. Hydrol. 201 (1-4), 120–137.
Memari, S.S., Bedekar, V.S., Clement, T.P., 2020. Laboratory and numerical investigation of saltwater intrusion processes in a circular island aquifer. Water Resour. Res. 56 (2) e2019WR025325.
Motz, L.H., 1992. Salt-water upconing in an aquifer overlain by a leaky confining bed. Groundwater 30 (2), 192–198.
Muskat, M., 1938. The flow of homogeneous fluids through porous media. Soil Sci. 46 (2), 169.
Oswald, S.E., Scheidegger, M.B., Kinzelbach, W., 2002. Time-dependent measurement of strongly density-dependent flow in a porous medium via nuclear magnetic resonance imaging. Transp. Porous Media 47 (2), 169–193.
Piscopo, V., Formica, F., Lana, L., Lotti, F., Pianese, L., Trifuoggi, M., 2020. Relationship between aquifer pumping response and quality of water extracted from wells in an active hydrothermal system: the case of the island of Ischia (Southern Italy). Water 12 (9), 2576.
Post, V.E.A., Bosserelle, A.L., Galvis, S.C., Sinclair, P.J., Werner, A.D., 2018. On the resilience of small-island freshwater lenses: evidence of the long-term impacts of groundwater abstraction on Bonriki Island, Kiribati. J. Hydrol. 564, 133–148.
Rathore, S.S., Tang, Y., Lu, C., Luo, J., 2020. A simplified equation of approximate interface profile in stratified coastal aquifers. J. Hydrol. 580, 124249. https://doi.org/10.1016/j.jhydrol.2019.124249.
Rathore, S.S., Zhao, Y., Lu, C., Luo, J., 2018a. Analytical analysis of the temporal asymmetry between seawater intrusion and retreat. Adv. Water Resour. 111, 121–131.
Rathore, S.S., Zhao, Y., Lu, C., Luo, J., 2018b. Defining the effect of stratification in coastal aquifers using a new parameter. Water Resour. Res. 54 (9), 5948–5957.
Reilly, T.E., Goodman, A.S., 1987. Analysis of saltwater upconing beneath a pumping well. J. Hydrol. 89 (3-4), 169–204.
Rubin, H., Pinder, G.F., 1977. Approximate analysis of upconing. Adv. Water Resour. 1 (2), 97–101.
Schmork, S., Mercado, A., 1969. Upconing of fresh water—sea water interface below pumping wells, field study. Water Resour. Res. 5 (6), 1290–1311.
Schneider, J.C., Kruse, S.E., 2006. Assessing selected natural and anthropogenic impacts on freshwater lens morphology on small barrier Islands: Dog Island and St. George Island, Florida, USA. Hydrogeol. J. 14 (1-2), 131–145.
Stoeckl, L., Houben, G., 2012. Flow dynamics and age stratification of freshwater lenses: experiments and modeling. J. Hydrol. 458-459, 9–15.
Stoeckl, L., Houben, G.J., Dose, E.J., 2015. Experiments and modeling of flow processes in freshwater lenses in layered island aquifers: analysis of age stratification, travel times and interface propagation. J. Hydrol. 529, 159–168.

Stoeckl, L., Walther, M., Graf, T., 2016. A new numerical benchmark of a freshwater lens. Water Resour. Res. 52 (4), 2474–2489.
Strack, O.D.L., 1972. Some cases of interface flow towards drains. J. Eng. Math. 6 (2), 175–191.
Tang, Y., Singh Rathore, S., Lu, C., Luo, J., 2020. Development of groundwater lens for transient recharge in strip islands. J. Hydrol. 590, 125209.
Vacher, H., 1988. Dupuit-Ghyben-Herzberg analysis of strip-island lenses. Geol. Soc. Am. Bull. 100 (4), 580–591.
Voss, C.I., Provost, A.M., 2002. SUTRA: A model for 2D or 3D saturated-unsaturated, variable-density ground-water flow with solute or energy transport.
Werner, A.D., Jakovovic, D., Simmons, C.T., 2009. Experimental observations of saltwater up-coning. J. Hydrol. 373 (1-2), 230–241.
Wirojanagud, P., Charbeneau, R.J., 1985. Saltwater upconing in unconfined aquifers. J. Hydraul. Eng. 111 (3), 417–434.
Yan, M., Lu, C., Werner, A.D., Luo, J., 2021. Analytical, experimental, and numerical investigation of partially penetrating barriers for expanding island freshwater lenses. Water Resour. Res. 57 (3) e2020WR028386.
Zhang, H., Hocking, G.C., 1996. Withdrawal of layered fluid through a line sink in a porous medium. ANZIAM J. 38 (2), 240–254.
Zhang, H., Hocking, G.C., Seymour, B., 2009. Critical and supercritical withdrawal from a two-layer fluid through a line sink in a partially bounded aquifer. Adv. Water Resour. 32 (12), 1703–1710.
Zhou, Q., Bear, J., Bensabat, J., 2005. Saltwater upconing and decay beneath a well pumping above an interface zone. Transp. Porous Media 61 (3), 337–363.